Mathematical Biosciences and Engineering

MBE, 19(9): 9335–9356.
DOI: 10.3934/mbe.2022434
Received: 01 May 2022
Revised: 05 June 2022
Accepted: 12 June 2022
Published: 27 June 2022

http://www.aimspress.com/journal/MBE

Research article

Fault feature extraction and fusion method for AUV with weak thruster fault based on variational mode decomposition and D-S evidence theory

Dacheng Yu, Mingjun Zhang, Xing Liu* and Feng Yao

College of Mechanical and Electrical Engineering, Harbin Engineering University, Harbin, 150001, China

* **Correspondence:** Email: liuxing0724@hrbeu.edu.cn.

Abstract: This study investigated the fault feature extraction and fusion problem for autonomous underwater vehicles with weak thruster faults. The conventional fault feature extraction and fusion method is effective when thruster faults are serious. However, for a weak thruster fault, that is, when the loss of effectiveness of thrusters is less than 10%, the following two problems occur if the conventional method is used. First, the ratio of fault features to noise features is small. Second, there is no monotonic relationship between the fusion fault features fused by the conventional method and the fault severity. In this paper, the following two methods are proposed to solve this problem: 1) Fault-feature extraction method. Based on negentropy, this method improves the evaluation index of the parameter optimization of the modified variational mode decomposition and finally enhances the fault features extracted by the modified Bayesian classification algorithm. 2) Fault-feature fusion method. To create a monotonic relationship between the fusion fault features and fault severity, this method expands the number of original signals of the traditional fusion method based on D-S evidence theory, improves the focus element of the traditional fusion method, and adopts the strategy of double fusion. Finally, the effectiveness of the proposed method was verified by pool-experiment results on Beaver II prototype.

Keywords: autonomous underwater vehicle; thruster; weak fault; fault feature extraction; fault feature fusion

1. Introduction

Autonomous underwater vehicles (AUV) play a critical role in a wide variety of underwater

missions such as military areas [1], seabed terrain scanning [2], underwater search [3], submarine pipeline inspection [4], underwater pollution detection [5], and marine resource development [6]. Because AUVs operate in a marine environment without cables or human interference, safety is a vital issue for AUVs [7-9]. As the most important power component of AUV, faults mainly occur in thrusters [10]. Research on the fault diagnosis technology of thrusters is of great significance and practical value for improving the safety of AUVs [11].

Most thruster faults in the early stages are weak, that is, their loss of effectiveness is relatively less [12]. If a thruster fault can be diagnosed at the early stage, it can give more time to guarantee the safety of AUVs [12]. With the acceleration of marine resource development, the study of weak fault diagnosis for AUV thrusters has become one of the current research hotspot [13].

The process of thruster fault diagnosis includes the following four steps [12,13]: fault feature extraction, fault feature fusion, fault detection, and fault severity identification. This study investigated a method of fault feature extraction and fusion for AUVs with weak thruster faults.

(1) Fault Feature Extraction

Data-driven feature-extraction methods are widely used. Currently, typical data-driven-based fault feature extraction methods include wavelet decomposition [14], empirical mode decomposition [15], neural networks [16], and manifold learning [17]. These methods have achieved good performance in feature extraction of serious thruster faults. No uniform standard exists for weak faults. In AUV fault diagnosis, a fault severity of less than 10% is generally regarded as weak [12,13]. Compared with serious thruster faults (loss of effectiveness of thrusters >10%), the fault feature is relatively small, and there is an overlap between the noise and fault features in the frequency domain for the weak thruster fault (loss of effectiveness of thrusters $\leqslant$10%) [13]. Therefore, it is difficult to directly use the typical fault feature extraction method to obtain a good performance for the fault feature extraction of weak thruster faults. Based on the aforementioned analysis, we used the method of combining wavelet and modified Bayesian algorithm (WMB) [14] to extract fault features. It was found that the ratio of fault features to noise features extracted using the WMB method was small.

Dragomiretskiy et al. [18], in 2014, proposed a new adaptive signal-processing method, called variational mode decomposition (VMD), based on the concepts of the Hilbert transform and Wiener filter. Because the Wiener filter has strong noise resistance, the VMD method has outstanding performance in noise reduction and feature extraction [19]. For example, Li et al. [20] proposed an adaptive denoising method based on VMD that could effectively eliminate the influence of noise and accurately extract the mode component of the water supply pipeline leakage signal from mixed noise. Yan et al. [21] used the excellent performance of VMD in feature extraction to realize the fault diagnosis of a bearing outer race. Zhao et al. [22] proposed a method called modified VMD (MVMD) for the adaptive selection of VMD parameters based on permutation entropy (PE), which has strong denoising and adaptive capabilities and has achieved good results in the fault diagnosis of rotating machinery. Because of the performance of the VMD method in feature extraction and noise reduction, we applied this method to extract the fault features of the thrusters.

(2) Fault Feature Fusion

Conventional fault fusion methods include the D-S evidence theory [23], fuzzy theory [24], and neural networks [25]. For example, Zhang et al. [23] proposed a fault feature fusion method based on D-S evidence theory for an AUV with a serious thruster fault, which effectively enhanced the ratio of fault features to noise features. Zhu et al. [24] used a fuzzy cerebellar model neural network based on

credit allocation to realize information fusion and fault identification of thrusters in underwater vehicles. Xiang et al. [25] used the Mamdani fuzzy neural network to realize the fusion of multi-sensor information for risk analysis and safety decision making for underwater vehicles. The purpose of fault feature fusion is to enhance the ratio of fault features, especially weak fault features, to noise features, and provide necessary data support for fault identification and safety decision making. The monotonicity between the fusion fault feature and fault severity is a prerequisite to ensure the accuracy of the subsequent fault severity identification. In recent years, we have developed monotonicity between the fusion fault feature and fault severity. For serious fault feature fusion of serious faults, we proposed a D-S evidence theory-based fault feature fusion method for an AUV with a serious thruster fault, which can effectively enhance the ratio of fault features to noise features and the monotonicity between the fusion fault feature and fault severity [23]. However, when the D-S evidence theory-based fault feature fusion method in [23] was used to fuse weak fault features, there was no monotonic relationship between the fusion fault feature and fault severity.

Based on the aforementioned analysis, we proposed a fault feature extraction and fusion method. The major contributions of this study are as follows:

(a) A novel and complete method was developed based on VMD and D-S evidence theory, consisting of a fault feature extraction and fault fusion methods. In this study, we focused on the problem of a small ratio of fault features to noise features extracted by WMB methods. To prepare for the subsequent fault severity identification, we conducted a preliminary study on the problem of no monotonic relationship between the fusion fault features and fault severity obtained by the traditional D-S evidence theory methods.

(b) A feature extraction method for weak thruster faults based on the modified MVMD and modified Bayesian algorithm (MB) was proposed. This method aimed at the problem of a small ratio of fault features to noise features extracted using the WMB method. We first investigated the difficulty of MVMD method in extracting the fault features of the AUV thruster. Based on the above reasons, we proposed a new method called modified MVMD, in which we substituted negentropy for PE to judge the levels of non-Gaussian modes and the noise levels of the modes. Finally, the modified-MVMD and MB were combined to extract fault features.

(c) A fault feature fusion method for weak thruster faults based on D-S evidence theory was proposed. This method is aimed at the problem of no monotonic relationship between the fusion fault feature obtained by the D-S evidence theory and fault severity. On the one hand, we defined the focus element from the perspective of the time interval. On the other hand, we fused all signals except the surge velocity signal based on the D-S evidence theory and then fused the surge velocity signal with the fusion results of other signals.

(d) The effectiveness of the proposed method was verified by pool-experiment results on a Beaver II AUV.

The remainder of this paper is organized as follows. Section 2 describes the modified feature extraction method for weak thruster faults based on the modified MVMD and MB. Section 3 presents an improved fault feature fusion method for weak thruster faults based on the D-S evidence theory. In Section 4, the research steps and block diagram of the fault feature extraction and fusion methods are presented. In Section 5, experiments conducted to verify the effectiveness of the proposed method are presented. Finally, conclusions are drawn in Section 5.

2. Fault feature extraction method

Aiming at the problem of a small ratio of the fault feature to the noise feature extracted, a method

improved by MVMD is proposed in this section, called modified MVMD. This section describes the modified fault feature extraction method based on modified MVMD and MB in detail after briefly describing the shortcomings of the MVMD method in weak fault feature extraction.

2.1. Problems and cause analysis of using MVMD method

Owing to its powerful ability of noise reduction and self-adaption, the MVMD method has achieved good performance in fault diagnosis for rotating machinery such as bearings [22]. By directly using the combination method of MVMD and MB (MVMD-MB) to extract the features of the weak thruster fault, the ratio between the fault features and noise features still cannot satisfy the requirements of fault diagnosis, although this ratio is slightly increased.

(1) Problem statement

In the study of weak fault feature extraction of thrusters based on MVMD-MB, the problem found in this paper is stated as follows. Compared with the WMB method, the ratio between the fault features and noise features extracted by the MVMD-MB method has insignificantly increased, which cannot meet the requirements of subsequent fault diagnosis.

(2) Cause analysis

In the MVMD-MB method, the main function of MVMD is noise reduction. It is considered that the mode with a larger PE value has a higher noise content in the MVMD method. The main idea was to gradually reduce noise by deleting the modes with the highest PE value. Because the noise signal is random, all types of symbol sequences appear in the process of calculating the PE value of the noise signal, but the corresponding probability is relatively small. This causes the PE value of the noise signal to be relatively high. Therefore, deleting modes with high PE values can reduce noise. In principle, the MVMD method has a good effect on noise reduction in fault feature extraction of rotating machinery. However, in contrast to the fault features of rotating machinery with periodic changes, the thruster fault feature in this study appears only once under the action of the closed-loop control system. Therefore, the occurrence probability of symbol sequences corresponding to the thruster fault feature is much smaller than that of rotating machinery. The MVMD method reduces noise from the angle of low occurrence probability of the symbol sequence. Owing to the low occurrence probability of thruster fault features in this study, it is easy to remove events with low occurrence probability, such as noise, which ultimately leads to a poor noise reduction effect.

2.2. Modified fault feature extraction method

Based on the cause analysis in Section 2.1, a modified fault feature extraction method is proposed in this subsection. This section explains the basic idea of this method, the difference between this and MVMD-MB methods, and the implementation process of this method.

2.2.1. Basic idea

(1) Introduce negentropy into MVMD

The probability density distribution of useful feature signals is primarily non-Gaussian, whereas

that of useless noise signals is Gaussian. The central limit theorem states that the probability density function of the sum of multiple random signals approaches a Gaussian distribution [26]. Therefore, the stronger the non-Gaussianity of the signal, the lower its noise content and the easier the fault feature information to be extracted [26]. Negentropy is an effective method for measuring non Gaussianity. It measures non-Gaussianity by measuring the similarity of the probability density distribution between the measured signal and noise signal. In recent years, negentropy has achieved good results in the noise reduction and feature extraction of weak signals [27-30]. Inspired by the above characteristics of negentropy, we introduced negentropy into MVMD. Specifically, negentropy replaced PE in MVMD and judged the levels of noise of the modes by judging the levels of non-Gaussian modes. According to the basic steps of MVMD [22], the mode with a low negentropy value was continuously deleted to achieve noise reduction.

(2) Theoretical Analysis

The modified extraction method deletes high-noise modes by negentropy from the perspective of a Gaussian distribution and the overall statistical characteristics of a signal. By contrast, MVMD deletes the high-noise mode from the occurrence probability of the local symbol sequence in a certain mode of the signal. Negentropy can avoid the problem of easy deletion of fault features as noise signals by PE method and can effectively preserves weak fault features.

2.2.2. Difference between modified extraction method and MVMD-MB

The flow charts of the modified extraction method are shown in Figure 1.

As shown in Figure 1, steps A, C, and D of the modified extraction method are the same as those of the MVMD-MB method [22,23]. In step B, the MVMD-MB method adopts the PE method to obtain the entropy value of each mode and target function (TF).

According to Figure 1, the process of the modified extraction method is as follows.

A. Initialization. The initial mode number, center frequency, and balancing parameters of the VMD are determined to obtain the initial mode set.

B. VMD parameter optimization. First, the negentropy of each mode is calculated. The modes are then sorted according to the entropy value. Finally, MTF is used as the criterion to obtain the optimal mode number and balancing parameter using the optimization method in MVMD.

C. Noise reduction. First, the original signal is decomposed by VMD according to the optimal mode number and balancing parameter. Next, the residual modal is deleted. Finally, the signal is reconstructed to achieve noise reduction.

D. Fault-Feature Extraction. The MB method is used to extract the fault features of the noise-reduced signal.

Difference between the modified extraction method and MVMD-MB. Compared to MVMD-MB, in step B, the modified extraction method improved the followings. 1) The modes were sorted by the negentropy of each mode. 2) The TF of MVMD-MB was improved according to negative entropy, and the modified TF (MTF) was used as the judgment index to determine the optimal parameters.

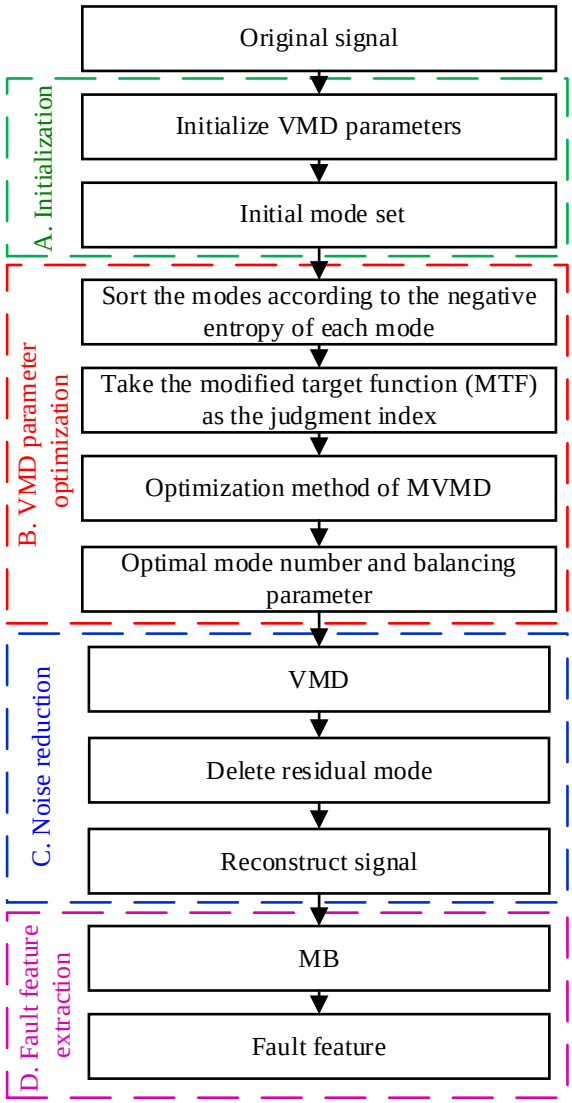

Figure 1. Flow chart of the modified extraction method.

2.3. Implementation process of modified extraction

Because steps A, C, and D of the modified extraction method were the same as those of the MVMD-MB [22,23], we will not repeat them. The improvements in Step B are described in detail below.

(1) Entropy of each mode

Negentropy theory was introduced to measure the noise levels by judging the non-Gaussian levels of each mode. The formula for calculating negentropy is as follows [26]:

$$J(y) = H(y_{gauss}) - H(y) \tag{1}$$

where y_{gauss} is a Gaussian random variable of the same covariance matrix as y. $H(\cdot)$ is the differential entropy of a random vector y with density $f(y)$, and is defined as [26]

$$H(y) = -\int f(y)logf(y)dy \tag{2}$$

It is computationally difficult to calculate the negentropy because it depends on the prior probability distribution of random variables and other factors. Approximations are generally adopted to obtain the estimated value of negentropy using the following formula [26]:

$$J(y) \approx [E\{G(y)\} - E\{G(v)\}]^2 \tag{3}$$

where v is a Gaussian variable with zero mean and unit variance (i.e., standardized). The mean and unit variance of variable y are both zero, $E(\cdot)$ is the expectation function; $G(\cdot)$ is a non-quadratic function.

According to the literature [26], $G(\cdot)$ in this paper is as follows:

$$G(u) = -exp\left(-\frac{u^2}{2}\right) \tag{4}$$

(2) To obtain MTF

After the introduction of negentropy, to match the TF with negentropy, this study improved the TF in MVMD based on negentropy to obtain an MTF. The MTF formula is as follows:

$$MTF(f, U) = \frac{NE(fres)}{\beta_1 J(frecon) + \beta_2 Orth + \beta_3 ELR} \tag{5}$$

where *f*, *frecon*, and *fres* represent the original signal, reconstructed signal as the sum of all modes, and residual part of the decomposition, respectively. β_i, i={1, 2, 3} are the weights of the different components that construct the denominator and are used to evaluate the contribution of each index to the final result. *ELR* denotes the ratio of the energy of the reconstructed signal to that of the original signal, and the larger the value, the lower the signal loss. The formula used is as follows:

$$ELR = \frac{energy(frecon)}{energy(f)} \tag{6}$$

where *Orth* denotes the orthogonality between the reconstructed and original signals. The higher the orthogonality value, the higher is the correlation between the two vectors. The formula used is as follows [22]:

$$Orth = \frac{frecon \cdot f}{|frecon| \cdot |f|} \tag{7}$$

Brief summarization of Section 2. Aiming at the problem of a small ratio of fault and noise features extracted by the WMB, this paper proposes a modified extraction method, which is verified by experimental results in Section 4.

3. Fault feature fusion method

Aiming at the problem of no monotony between fault feature after fused based on D-S evidence theory and fault severity for AUV with weak thruster fault, an improved fault feature fusion method based on D-S evidence theory is proposed in this paper. This section explains the problems of the D-S evidence theory-based fusion method for weak-fault feature extraction. Then, it analyzes the causes of

these problems. Finally, it explains the ideas and implementation steps of the improved fusion method based on D-S evidence theory.

3.1. Problem statement

First, the fault feature extracted as described in Section 2 is used to extract the fault features from the surge velocity, main thruster control, lateral thrust control, and yaw angle signals. Then, these different fault features from different signals are fused to achieve a monotonic relationship between the fused fault feature and magnitude of the thruster fault and to further increase the ratio of the fault feature to the noise feature. This was the objective of the present study.

The D-S evidence theory is a conventional method of feature fusion. The use of the D-S evidence theory in fusing the different fault features from different signals results in no monotonic relationship between the fused fault feature and magnitude of thruster fault for AUV with serious thruster fault (hereinafter referred to as "non-monotonic problem") [23]. To solve this problem, a fusion method based on the peak area energy method was developed in our previous research based on the D-S evidence theory [23]. The method in [23] achieved a monotonic relationship between the fusion fault feature and fault severity for AUV with serious thruster faults. However, according to the method in [23], a monotonic relationship cannot be obtained for AUV with weak thrusters.

3.2. Cause analysis

(1) Simple description of the D-S evidence theory-based fusion method.

To easily explain the improved feature fusion method, we described the process of the traditional fusion method based on the D-S evidence theory. First, the focus element is defined as an event in which a fault occurs at one beat of a signal. The value of the focus element is the probability of fault occurrence at this beat. Subsequently, the mass functions from different feature signals are fused according to Dempster's rule [31] to obtain the final fault feature.

(2) Causes of nonmonotonic problems

1) According to the experimental data, the beat numbers corresponding to the maximum value of the focus element were different among these feature signals. Therefore, if the focus element is defined from the perspective of each beat number, according to Dempster's rules, the simultaneous multiplication of maximum value of the focus element for all feature signals cannot be guaranteed. Furthermore, it sometimes does not let the fused fault feature increase with fault severity, that is, a non-monotonic problem.

2) In the feature fusion, the mass function is obtained by calculating the fault occurrence probability of the fault feature signal at each beat. The fault occurrence probability at a certain beat is calculated by dividing the value of the fault feature signal at that beat by the sum of the values of the signal at all beats. For weak faults, each fault feature is significantly affected by sensor noise and external disturbances. When the maximum value of the fault feature signal is divided by the sum of the values of the fault feature signal at all times, the result decreases. Moreover, when the magnitude of the thruster fault increases monotonically, the sum of the values of the fault feature signal at all times changes irregularly. Therefore, it is impossible to guarantee a monotonic relationship between the fault features and fault severity.

3.3. Improved fault feature fusion method

This section explains the basic ideas and implementation process of the improved method.

(1) Basic ideas

According to the analysis in subsection 3.2, this study improved two aspects of the D-S evidence theory-based fusion method, and the basic ideas of improvement are as follows.

1) Define the focus element from the perspective of time interval

The focus element of the improved fusion method in this study was defined from the perspective of time interval. By selecting an appropriate time interval, the maximum value of the fault feature signal, out of multiple signals, is guaranteed to be in the same time interval to obtain the fusion feature by the maximum fault occurrence probability of multiple feature signals.

2) Add a second fusion

In this study, it was found that the surge velocity signal plays a leading role in the process of fault feature fusion. When the thruster has a weak fault, the maximum value of the surge velocity fault feature signal becomes smaller in feature fusion after the basic probability assignment of the D-S evidence theory. As a result, the leading role of the surge velocity signals is weakened after fusion. To solve the above problem, the fault feature signal of surge velocity does not participate in the fusion based on the D-S evidence theory and fuses with other feature signals using another method.

(2) Implementation of improved fusion method

The flow chart of the improved fusion method is shown in Figure 2.

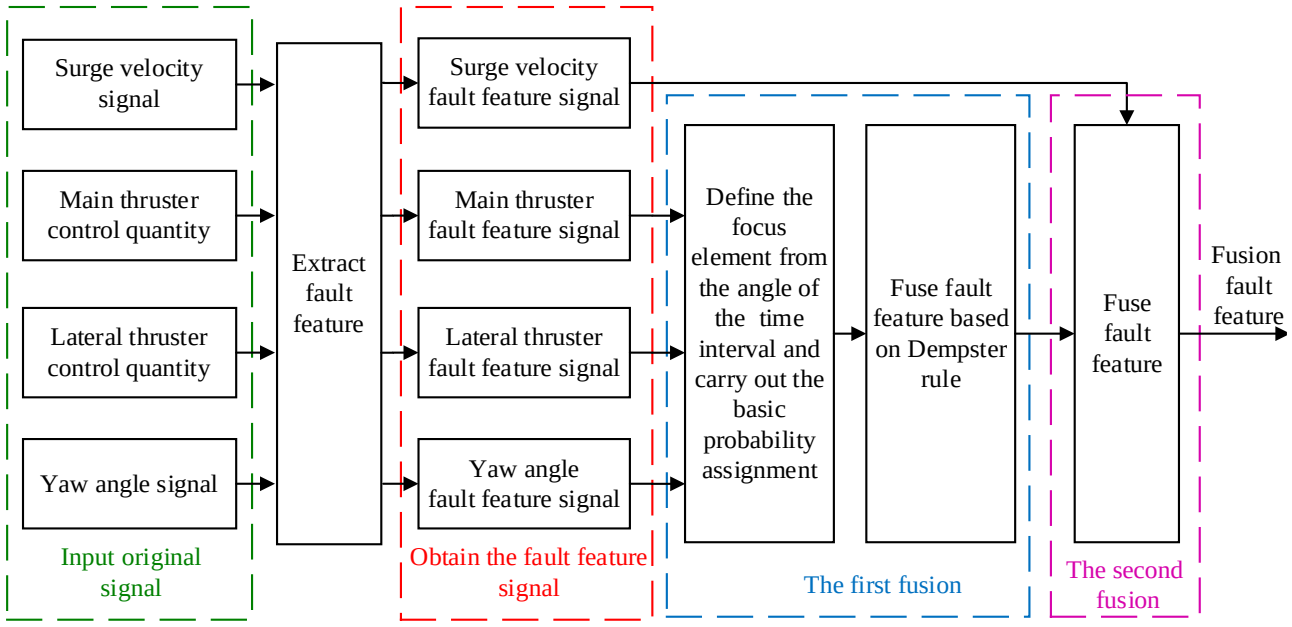

Figure 2. Flow chart of the improved fusion method.

The improved fusion method is implemented in the following steps.

1) Fault features extraction

These signals, including the right main thruster control, lateral thruster control, and yaw angle

signals, were differentiated first. Then, their corresponding results, together with the surge velocity signal, were used to extract the fault features according to the modified extraction method given in Section 2.

2) Focus element and basic probability assignment

This step differs from the D-S evidence theory-based fusion method, and its specific content is as follows:

① The feature signal is divided into multiple time intervals according to a fixed length *N*, and the fault feature signal $X = \{x(1), x(2), \cdots x(3)\}$ is divided into N_2 time intervals from left to right, and the fault feature vector y_k of each time interval is obtained. The formula for y_k is as follows.

$$y_k = \{x(k), x(k+1), \cdots, x(k+N-1)\} \tag{8}$$

where $k = 1, 2, 3, \cdots, N_2$.

Determination of fixed-length N. After statistics on the beats of the maximum value of all feature signals of all fault severities, it is found that when the maximum value of the fault feature of different signals with the same fault severity appears, it is distributed in the time interval of approximately 20 beats, which is called the maximum value distribution interval, the location of which varies with the fault severity. To fuse the maximum value of the fault feature signal of multiple signals, the time interval considered in this study is 45 beats long (greater than twice the length of the maximum value distribution interval) such that the maximum values of the fault feature signals of different signals are located in the same interval.

② The focus element is defined. Consider the event where a fault occurs in the *k*-th time interval as the focus element A_k to build the identification framework $\Theta = \{A_1, A_2, \cdots, A_n\}$.

③ Basic probability assignment was achieved. In the D-S evidence theory, a mass function is also called a basic probability assignment. According to (9), the mass function of the fault feature signals of the main thruster control, lateral thruster control, and yaw angle signals is obtained.

$$m(A_k) = \frac{d(k)}{\sum_{j=1}^{N_2} d(j)} \tag{9}$$

where $d(k)$ is the maximum value of fault feature vector y_k in the *k*-th time interval.

3) First fusion: based on Dempster's rule

As this step is the same as the D-S evidence theory-based fusion method [14,31], the content of this step is omitted here. In the first fusion, the mass function of other signals is fused based on the D–S evidence theory, and the fault feature signal of the surge velocity does not participate in it.

4) Second fusion

This step differs from the D-S evidence theory-based fusion method, and its specific content is as follows:

①The fusion mass function $m_F(A_k)$ obtained by the first fusion is fused with the surge velocity fault feature signal $S(t)$ for the second time to obtain the fusion fault fusion signal $M_F(t)$. The fusion fault feature signal is obtained according to Eqs. (10) and (11).

$$M_F(t) = S(t) \cdot \omega(t) \tag{10}$$

$$\omega(t) = m_F(A_1) + \sum_{i=1}^{n} [m_F(A_{i+1}) - m_F(A_i)] \cdot U(t - a_i) \tag{11}$$

where $a_i = N_1 \cdot i$; $0 < t < N_1 \cdot N_2$, $t \in N$; $U(t)$ is the unit step function.

②The maximum value of the fusion fault feature signal $M_F(t)$ is considered as the thruster fusion fault feature F. The formula for F is as follows:

$$F = \max M_F(t) \tag{12}$$

Briefly summarize section 3. Because of the "non-monotonic" problem of the D-S evidence theory-based fusion method, this paper proposes an improved feature fusion method based on the D-S evidence theory, which will be verified experimentally in Section 5.

4. Fault feature extraction and fusion method

Based on the methods proposed in Sections 2 and 3, a block diagram of the fault feature extraction and fusion method proposed in this study is shown in Figure 3.

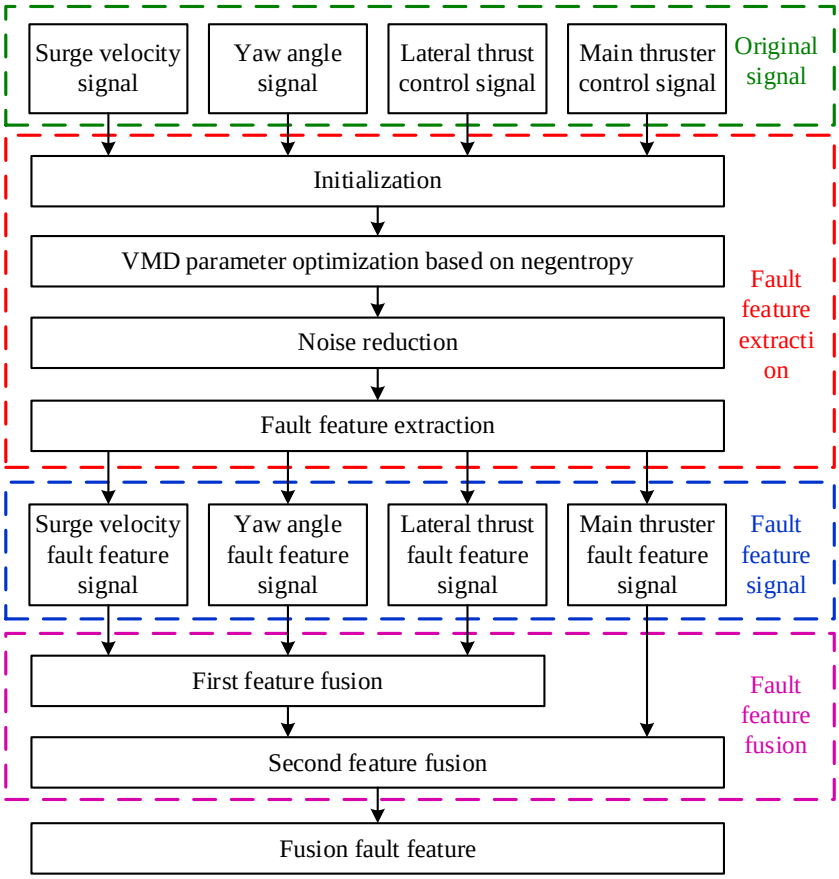

Figure 3. Flow chart of Fault feature extraction and fusion method.

According to Figure 3, the specific steps are as follows:

1) Original signal. The signals studied in this paper are the surge velocity, yaw angle, lateral thrust control, and main thruster control signals.

2) Initialization. The initial mode number, center frequency, and balancing parameters of VMD were determined to obtain the initial mode set.

3) VMD parameter optimization based on negentropy. First, the negentropy of each mode was calculated. The modes were then sorted according to the entropy value. Finally, MTF was used as the criterion to obtain the optimal mode number and balancing parameter using the optimization method in MVMD.

4) Noise reduction. First, the original signal was decomposed by VMD according to the optimal mode number and balancing parameter. Next, the residual mode was deleted. Finally, the signal was reconstructed to achieve noise reduction.

5) Fault feature extraction. MB method was used to extract the fault feature of the noise reduced signal.

6) First feature fusion. This fusion was based on the D-S evidence theory. First, the focus element was determined as the fault occurred in this time interval. Subsequently, a basic probability was assigned. Finally, the fusion was based on Dempster's rule.

7) Second feature fusion. The fusion mass function of the first feature fusion was fused with the surge velocity signal to obtain the fusion fault feature.

5. Experiments verification

To verify the effectiveness of the modified fault feature extraction method and improved fault feature fusion method, a Beaver II AUV experimental prototype was used to conduct a pool experiment.

5.1. Experimental setup and original signal

Beaver II was commanded to track surge velocity with 0.3 m/s in an experiment [14]. Beaver II is shown in Figure 4, and the experimental conditions are shown in Figure 5.

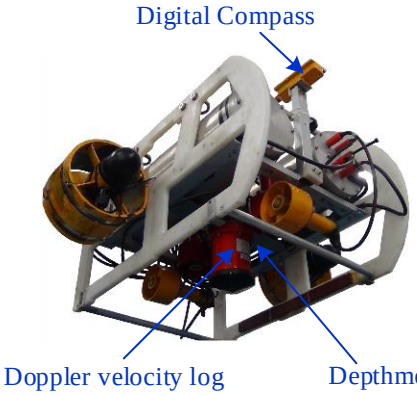

Figure 4. Beaver II AUV experimental prototype.

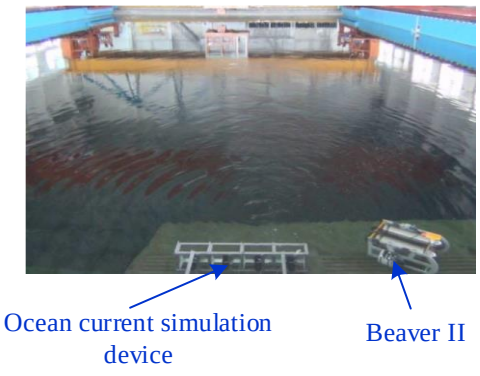

Figure 5. Experimental condition.

The sensor system of Beaver II was composed of a digital compass, Doppler velocity log, and depth meter, as shown in Figure 4. The Beaver II propulsion system was composed of six brush thrusters, as shown in Figure 6. The surge speed was controlled by thrusters HT3 and HT4. The heading was controlled by the thrusters HT1 and HT2. The depth was controlled by thrusters VT1 and VT2. The control system was based on a PID controller.

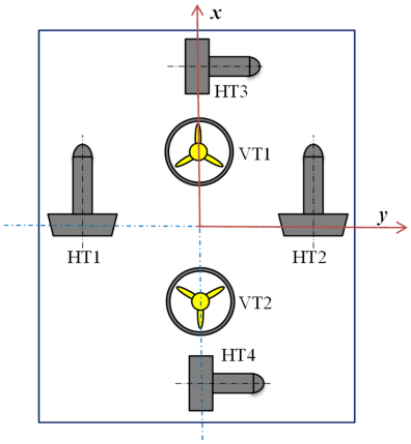

Figure 6. Thruster configuration of the Beaver II.

In the pool experiment, the target velocity of AUV was 0.3 m/s and the control period was 0.2 s. The AUV started in a static state and continued to accelerate until it reached the target speed. The AUV was then operated in a straight line at the target velocity. From the 250th beat, the soft fault simulation method [14] was used to simulate the left main thruster fault until the end of the experiment. The following cases with different thruster fault severities were simulated: 5%, 8%, 10%, 20%, 30%, and 40% loss of effectiveness in a single thruster. The experimental setup is shown in Figure 7.

(a) Beaver II is moving; (b) Beaver II is hovering.

Figure 7. Pool experimental.

Assuming the fault with a 5% loss of effectiveness as an example, the four original signals (surge velocity, yaw angle, lateral thrust control, and main thruster control signals) are shown in Figure 8.

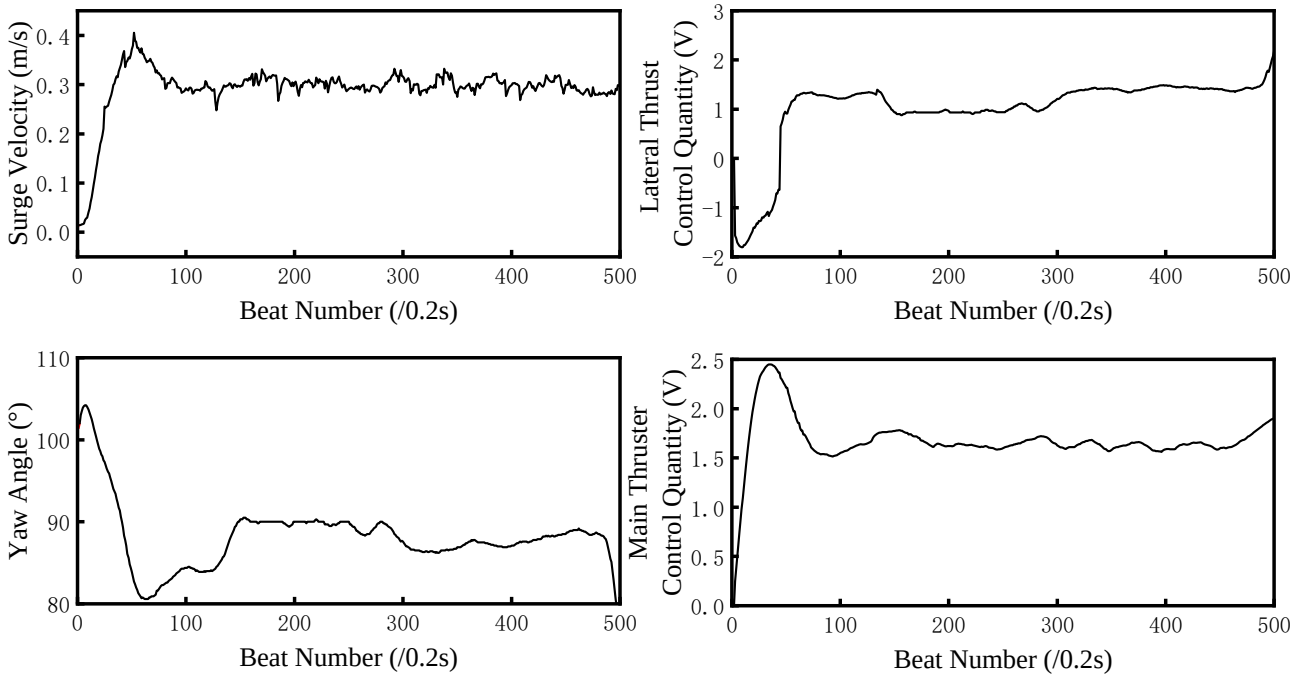

Figure 8. The original signals.

Analyzing Figure 8, the first 100 beats are the AUV start-up phase, and the velocity is steady at 0.3 m/s. Because this paper studied the fault diagnosis of the AUV thruster in steady-state operation, the start-up phase was ignored [14], that is, the experimental data of 201 to 400 beats were used for analysis.

5.2. Experimental verification of fault feature extraction

As the modified extraction method is a modified version of the WMB and MVMD-MB methods, this section presents a comparative experiment of these three methods to verify the effect of the modified extraction method. In addition, the effect of the modified extraction method on serious faults is verified.

5.2.1. Comparison for weak thruster fault

The modified extraction, MVMD-MB, and WMB methods were used to extract the fault features of the four original signals with a weak fault (the loss of effectiveness of the left main thruster was 5%, 8%, and 10%, respectively). Assuming the surge velocity signal with a 5% loss of effectiveness as an example, the fault feature extraction results for each method are shown in Figure 9.

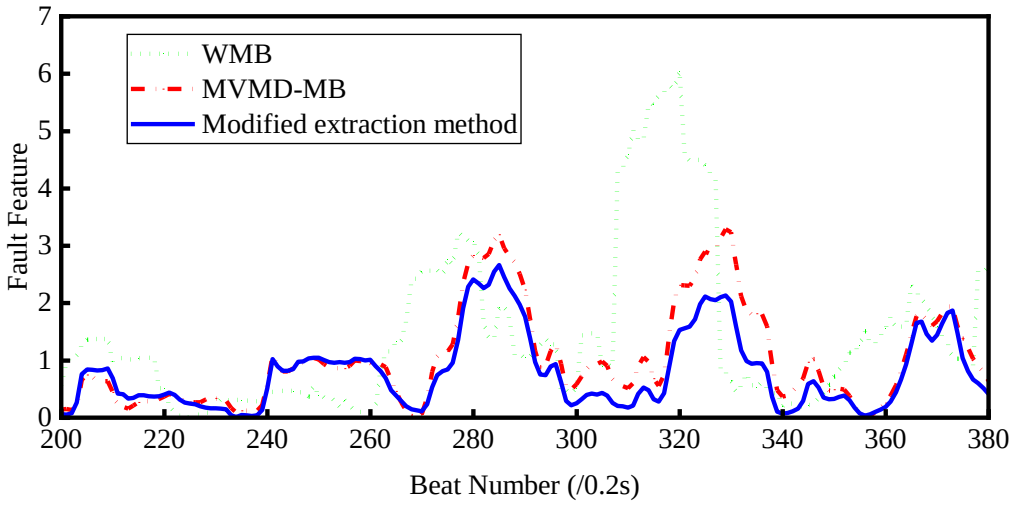

Figure 9. Feature extraction results of surge velocity signal with 5% loss of effectiveness.

To conveniently analyze the problem, the fault feature extraction results of surge velocity signals with 5%, 8%, and 10% loss of effectiveness are tabulated in Table 1.

Table 1. In the case of weak faults, feature extraction results of the surge velocity signal.

Fault severity	Index	WMB	MVMD-MB	Modified extraction method
5 %	Fault feature	3.20	3.10	2.66
	Noise feature	6.04	3.28	2.06
8 %	Fault feature	2.73	2.30	2.99
	Noise feature	1.77	1.61	1.80
10 %	Fault feature	3.88	3.15	3.56
	Noise feature	3.86	2.90	3.18

In subsequent fault detection and fault severity identification, the ratio of the fault feature to the noise feature was primarily used [12-14,23]. Therefore, the ratio of the fault feature value to the noise feature value was determined, as listed in Table 2.

Table 2. In the case of weak faults, the ratio of the surge velocity signal of each method.

Fault severity	WMB	MVMD-MB	Modified extraction method
5 %	0.53	0.95	1.29
8 %	1.54	1.43	1.66
10 %	0.99	1.09	1.11

The data in Table 1 are the fault feature values extracted from the curves in Figure 9. The ratio of the fault feature values to the noise feature values in Table 2 can be obtained only from Table 1. The data in Table 2 are discussed herein, and the data in Table 1 are for the intermediate process. Therefore, instead of analyzing Table 1, Table 2 was analyzed. According to Table 2, this study conducted a comparative analysis of the ratio of the fault feature to the noise feature.

(1) Comparison of the modified extraction and MVMD-MB methods

When the loss of effectiveness of the thrusters was 5%, 8%, and 10%, compared with the MVMD-MB method, the ratio of the fault feature to the noise feature of the modified extraction method increased by 35.79%, 16.08%, and 1.83%, respectively.

(2) Comparison of the modified extraction method and the WMB method

When the loss of effectiveness of the thrusters was 5%, 8%, and 10%, compared with the WMB method, the ratio of the fault feature to the noise feature of the modified extraction method increased by 143.40%, 7.80%, and 12.12%, respectively.

In conclusion, the above experimental results demonstrate that the proposed extraction method can identify faults with more than 5% fault severity. The proposed extraction method can effectively extract the fault features of weak faults with thruster fault severity between 5% and 10%, whereas MVMD-MB and WMB cannot effectively extract the fault features. Moreover, for weak faults with fault severities between 5% and 10%, the ratio of fault feature values to noise feature values is significantly increased compared with MVMD-MB and WMB, verifying the effectiveness of this method in the fault feature enhancement of weak faults.

5.2.2. Comparison for serious thruster fault

To verify the effect of the modified extraction method on serious thruster faults, the modified extraction, MVMD-MB, and WMB methods were used to extract the fault features of the four original signals from the AUV with three different thruster faults, including 20%, 30%, and 40% loss of effectiveness. Assuming the surge velocity signal with a 20% loss of effectiveness as an example, the fault feature extraction results for each method are shown in Figure 10.

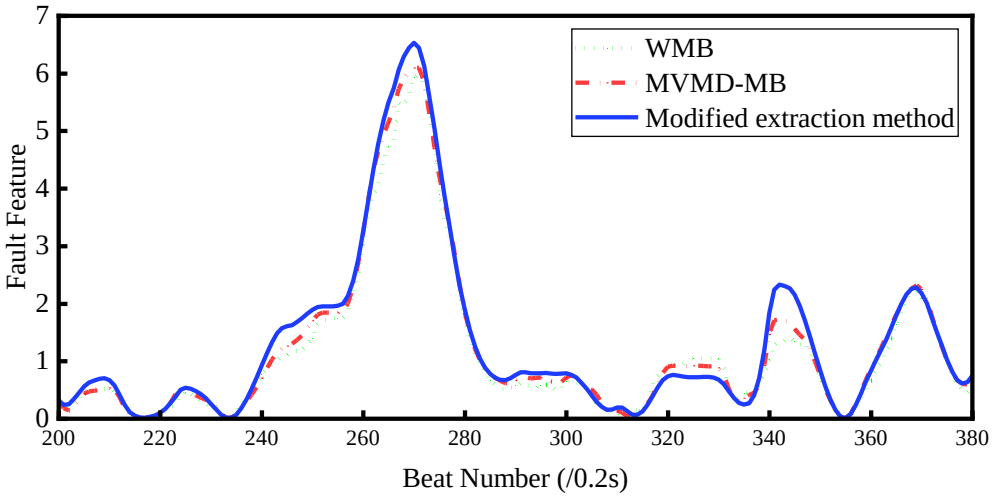

Figure 10. Feature extraction results of surge velocity signal with 20% loss of effectiveness.

Table 3. In the case of serious faults, the ratio of the surge velocity signal of each method.

Fault severity	WMB	MVMD-MB	Modified extraction method
20%	2.69	2.59	2.80
30%	3.10	3.35	3.63
40%	1.67	4.36	4.40

To analyze the problem conveniently, the ratio of the fault feature to the noise feature in the case of a serious fault is determined, as shown in Table 3.

The data in Table 3 were extracted from the curve shown in Figure 10. Therefore, Table 3 was analyzed instead of figure 10. According to Table 3, this study conducted a comparative analysis of the ratio of the fault feature to the noise feature.

(1) Comparison of the modified extraction and MVMD-MB methods

When the loss of effectiveness of the thruster was 20%, 30%, and 40%, compared with the MVMD-MB method, the ratio of the fault feature to the noise feature of the modified extraction method increased by 8.11%, 8.36%, and 0.92%, respectively.

(2) Comparison of the modified extraction and WMB methods

When the loss of effectiveness of the thruster was 20%, 30%, and 40%, compared with the WMB method, the ratio of the fault feature to the noise feature of the modified extraction method increased by 4.09%, 17.10%, and 221.17%, respectively.

In conclusion, the above experimental results show that the above three methods can effectively extract the fault features of strong faults with a thruster fault severity greater than 10%. However, compared with MVMD-MB and WMB, the ratio of fault feature values to noise feature values significantly increased for serious faults with fault severities greater than 10%, verifying the effectiveness of this method in fault feature enhancement of serious faults.

5.3. Experimental verification of fault feature fusion

Because the improved fault fusion method is improved on the D-S evidence theory-based fusion and peak region energy methods, this study conducted a comparative experiment of these three methods to verify the effect of the improved fusion method proposed in this study.

Based on the modified extraction method described in Section 4.2, the fault feature signals of the four original signals with different fault severities were obtained. Based on the above signals, the improved fusion method, the D-S evidence theory-based fusion method, and the peak area energy method are used to obtain the fusion fault feature with 5%, 8%, 10%, 20%, 30%, and 40% loss of effectiveness. The results are tabulated in Table 4.

Table 4. Fusion fault feature of thrusters obtained by each fusion method.

Fault severity	The D-S evidence theory-based fusion method	The peak area energy method	The improved fusion method
5%	0.094	0.794	1.712
8%	0.110	0.793	2.232
10%	0.082	0.429	3.119
20%	0.077	0.969	6.516
30%	0.087	0.996	7.239
40%	0.088	0.999	16.010

To conveniently analyze the problem, the mapping relationship between the fusion fault feature and fault severity obtained by the above three methods is shown in table 4, as shown in Figure 11.

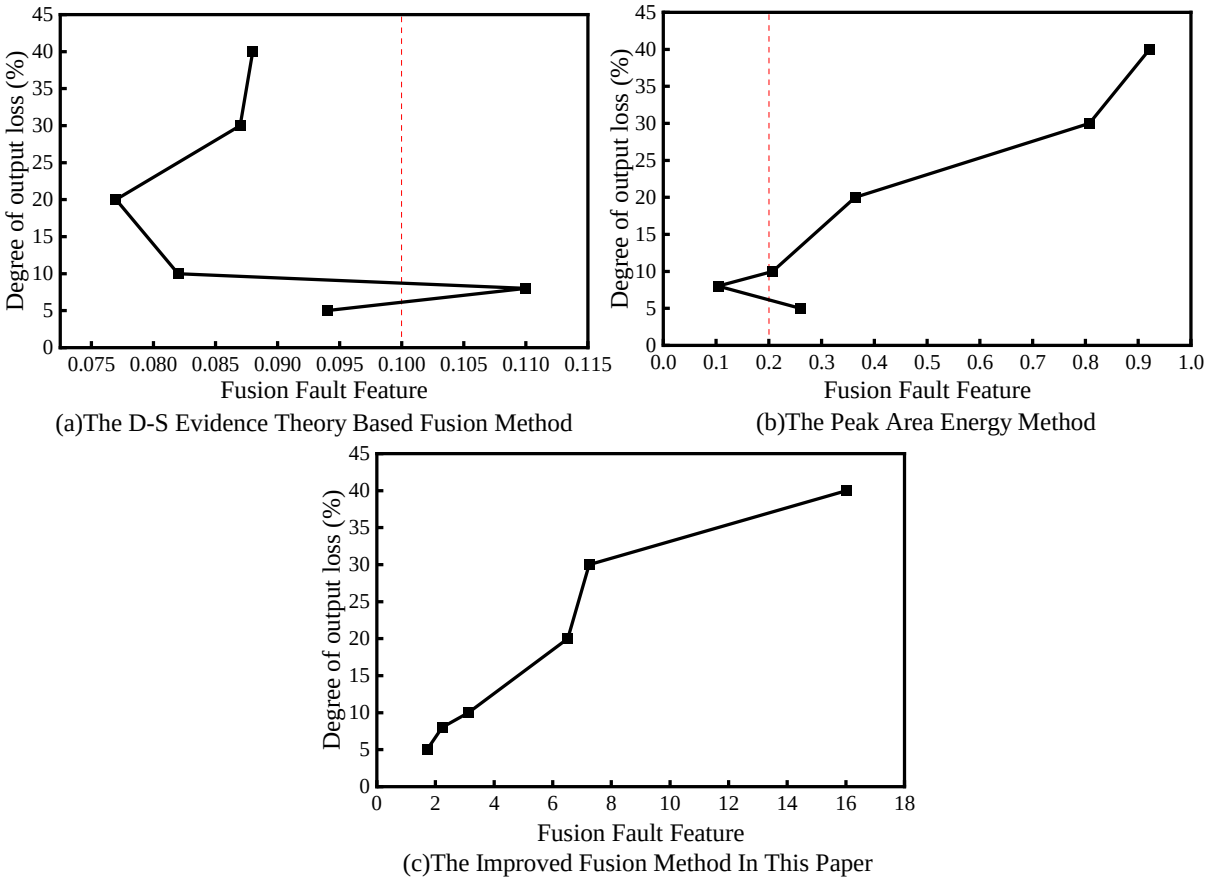

Figure 11. The mapping relationship between fusion fault feature and fault severity.

As shown in Figure 11, the monotonic relationship between the fusion fault feature and fault severity of each method was analyzed.

(1) Analysis of the experimental results of the D-S evidence theory-based fusion method

As shown in Figure 11 (a), for serious faults, the fusion fault features obtained by the D-S evidence theory-based fusion method showed a monotonic relationship with fault severity. As indicated by the red dotted line in Figure 11 (a), the fusion fault feature of 0.100 corresponded to two fault severities. This shows that for weak faults, the fusion fault feature obtained by the D-S evidence theory-based fusion method did not show a monotonic relationship with fault severity. Therefore, this method cannot solve the non-monotonic problem of weak faults and is only useful for serious faults.

(2) Analysis of the experimental results of the peak area energy method

As shown in Figure 11 (b), for serious faults, the fusion fault features obtained by the peak area energy method showed a monotonic relationship with fault severity. As shown by the red dotted line in Figure 11 (b), the fusion fault feature of 0.2 corresponded to two fault severities. This shows that for weak faults, the fusion fault feature obtained by the peak area energy method did not exhibit a monotonic relationship with fault severity. Therefore, this method cannot solve the non-monotonic problem of weak faults and is only useful for serious faults.

(3) Analysis of the experimental results of this improved fusion method

As shown in Figure 11 (c), for all faults with a fault severity greater than or equal to 5%, the fusion fault feature obtained by the improved fusion method in this study exhibited a monotonic relationship with the fault severity, that is, a fusion fault feature corresponded to a unique fault severity.

Therefore, the improved fusion method can solve the non-monotonicity problem of weak faults that the D-S evidence theory-based fusion method and peak area energy method cannot solve.

In conclusion, for serious faults, the above three methods can solve the nonmonotonic problem. In the case of a weak fault, if the fault severity is between 5% and 10%, the improved fusion method can solve the non-monotonicity problem, whereas the other two methods cannot solve the problem; if the fault severity is less than 5%, the above three methods are invalid. Because the thrusters studied in this paper belong to rotating machinery, the method in this paper can also be used as a reference for weak fault diagnosis of rotating machinery, such as bearings [32–34].

6. Conclusions

In this study, the problem of fault feature extraction and fusion for weak faults in AUV thrusters was investigated, including the research on feature enhancement of weak fault feature extraction based on MVMD and MB, and research on non-monotonicity of weak fault feature fusion based on D-S evidence theory.

When the thruster has weak faults, the ratio of the fault feature to the noise feature extracted using the WMB method is small. Although the MVMD-MB can slightly increase the ratio, the result cannot satisfy the requirement of the subsequent fault diagnosis. Therefore, this study proposed a modified fault feature extraction method for an AUV thruster. The pool experiment results showed that compared with the MVMD-MB and WMB methods, the modified extraction method significantly improved the ratio of fault features to noise features for weak faults. The results verified that the modified extraction method effectively enhanced fault features. Simultaneously, through experimental verification, it was found that the modified extraction method can also be applied to fault feature extraction for AUVs with serious thruster faults.

When the thruster has weak faults, there is a non-monotone relationship between the fusion fault feature obtained by the D-S evidence theory-based fusion method, wave peak region energy method, and fault severity. To solve this problem, in this paper, an improved thruster fault feature fusion method was proposed based on the D-S evidence theory. The pool experiment results of Beaver II showed that when the AUV thrusters had weak faults, there was a monotonic relationship between the fusion fault feature obtained by the improved fusion method in this study and fault severity.

This fault extraction and fusion method can identify faults with more than a 5% fault severity. This method can help the AUV judge the fault severity in the early stage of a fault, detect the fault in the early stage, and take measures in the early stage. It ensures the safety of an AUV and prevents serious development of the fault or even loss due to the fault. This method can accelerate the practical processing of AUV.

The data for this experiment were obtained at a fixed current intensity. In future research, we will further study the weak fault feature extraction method under different current intensities to adapt to complex marine environments.

Acknowledgment

This work was supported in part by the National Natural Science Foundation of China under Grant 51839004.

Conflict of interest

The authors declare there is no conflict of interest.

References

1. A. Hernandez-Sanchez, A. Poznyak, I. Chairez, O. Andrianova, Robust 3-D autonomous navigation of submersible ship using averaged sub-gradient version of integral sliding mode, *Mech. Syst. Signal Proc.*, **149** (2021), 107169. https://10.1016/j.ymssp.2020.107169
2. K. Krasnosky, C. Roman, D. Casagrande, A bathymetric mapping and SLAM dataset with high-precision ground truth for marine robotics, *Int. J. Robot. Res.*, **41** (2022), 12–19. https://10.1177/02783649211044749
3. X. Cao, H. Sun, L. Guo, Potential field hierarchical reinforcement learning approach for target search by multi-AUV in 3-D underwater environments, *Int. J. Control*, **93** (2020), 1677–1683. https://10.1080/00207179.2018.1526414
4. F. R. Wang, Z. Chen, G. B. Song, Smart crawfish: A concept of underwater multi-bolt looseness identification using entropy-enhanced active sensing and ensemble learning, *Mech. Syst. Signal Proc.*, **149** (2021), 107186. https://10.1016/j.ymssp.2020.107186
5. C. Lin, G. Han, T. Zhang, S. B. H. Shah, Y. Peng, Smart Underwater Pollution Detection Based on Graph-Based Multi-Agent Reinforcement Learning Towards AUV-Based Network ITS, *IEEE Trans. Intell. Transp. Syst.*, (2022). https://10.1109/tits.2022.3162850
6. H. Wang, L. Dong, W. Song, X. Zhao, J. Xia, T. Liu, Improved U-Net-Based Novel Segmentation Algorithm for Underwater Mineral Image, *Intell. Autom. Soft Comput.*, **32** (2022), 1573–1586. https://10.32604/iasc.2022.023994
7. S. Gao, B. He, F. Yu, X. Zhang, T. H. Yan, C. Feng, An abnormal motion condition monitoring method based on the dynamic model and complex network for AUV, *Ocean Eng.*, **237** (2021), 109472. https://10.1016/j.oceaneng.2021.109472
8. F. Liu, H. Tang, J. Luo, L. Bai, H. Pu, Fault-tolerant control of active compensation toward actuator faults: An autonomous underwater vehicle example, *Appl. Ocean Res.*, **110** (2021), 102597. https://10.1016/j.apor.2021.102597
9. Y. Liu, R. Bucknall, The angle guidance path planning algorithms for unmanned surface vehicle formations by using the fast marching method, *Appl. Ocean Res.*, **59** (2016), 327–344. https://10.1016/j.apor.2016.06.013
10. C. Zhu, B. Huang, B. Zhou, Y. M. Su, E. H. Zhang, Adaptive model-parameter-free fault-tolerant trajectory tracking control for autonomous underwater vehicles, *ISA Trans.*, **114** (2021), 57–71. https://10.1016/j.isatra.2020.12.059
11. P. Wu, C. A. Harris, G. Salavasidis, A. Lorenzo-Lopez, I. Kamarudzaman, A. B. Phillips, et al., Unsupervised anomaly detection for underwater gliders using generative adversarial networks, *Eng. Appl. Artif. Intell.*, **104** (2021), 104379. https://10.1016/j.engappai.2021.104379
12. T. Lv, Z. Y. Chen, F. Yao, M. J. Zhang, Fault feature extraction method based on optimized sparse decomposition algorithm for AUV with weak thruster fault, *Ocean Eng.*, **233** (2021), 109013. https://10.1016/j.oceaneng.2021.109013
13. W. X. Liu, Y. J. Wang, X. Liu, M. J. Zhang, Weak thruster fault detection for AUV based on stochastic resonance and wavelet reconstruction, *J. Cent. South Univ.*, **23** (2016), 2883–2895. https://10.1007/s11771-016-3352-1
14. M. Zhang, B. Yin, W. Liu, Y. Wang, Feature extraction and fusion for thruster faults of AUV with random disturbance, *J. HUAZHONG UNIV. SCI. TECHNO:NAT. SCI. ED.*, **43** (2015), 22–26 and 54. https://10.13245/j.hust.150605

15. J. Q. Li, J. Li, H. Y. Chen, Y. Zhang, Y. C. Xie. Propeller feature extraction of UUVs study based on CEEMD combined with symmetric correlation. In *2020 2nd International Conference on Computer Science Communication and Network Security (CSCNS2020)*, (2020), 02006. https://10.1051/matecconf/202133602006
16. D. S. Yang, Y. H. Pang, B. W. Zhou, K. Li, Fault Diagnosis for Energy Internet Using Correlation Processing-Based Convolutional Neural Networks, *IEEE Trans. Syst. Man Cybern. Syst.*, **49** (2019), 1739–1748. https://10.1109/tsmc.2019.2919940
17. R. Wang, H. Chen, C. Guan, W. Gong, Z. Zhang, Research on the fault monitoring method of marine diesel engines based on the manifold learning and isolation forest, *Appl. Ocean Res.*, **112** (2021), 102681. https://10.1016/j.apor.2021.102681
18. K. Dragomiretskiy, D. Zosso, Variational Mode Decomposition, *IEEE Trans. Signal Process.*, **62** (2014), 531–544. https://10.1109/tsp.2013.2288675
19. X. Jiang, J. Wang, C. Shen, J. Shi, W. Huang, Z. Zhu, et al., An adaptive and efficient variational mode decomposition and its application for bearing fault diagnosis, *Struct. Health Monit.*, (2020), 1–18. https://10.1177/1475921720970856
20. J. Li, Y. Chen, Z. H. Qian, C. G. Lu, Research on VMD based adaptive denoising method applied to water supply pipeline leakage location, *Measurement*, **151** (2020), 107153. https://10.1016/j.measurement.2019.107153
21. X. A. Yan, M. P. Jia, Application of CSA-VMD and optimal scale morphological slice bispectrum in enhancing outer race fault detection of rolling element bearings, *Mech. Syst. Signal Proc.*, **122** (2019), 56–86. https://10.1016/j.ymssp.2018.12.022
22. Y. J. Zhao, C. S. Li, W. L. Fu, J. Liu, T. Yu, H. Chen, A modified variational mode decomposition method based on envelope nesting and multi-criteria evaluation, *J. Sound Vibr.*, **468** (2020), 115099. https://10.1016/j.jsv.2019.115099
23. M. Zhang, B. Yin, X. Liu, J. Guo, Thruster fault identification method for autonomous underwater vehicle using peak region energy and least square grey relational grade, *Adv. Mech. Eng.*, **7** (2015), 1–11. https://10.1177/1687814015622905
24. D. Zhu, B. Sun, Information fusion fault diagnosis method for unmanned underwater vehicle thrusters, *IET Electr. Syst. Transp.*, **3** (2013), 102–111. https://10.1049/iet-est.2012.0052
25. X. B. Xiang, C. Y. Yu, Q. Zhang, On intelligent risk analysis and critical decision of underwater robotic vehicle, *Ocean Eng.*, **140** (2017), 453–465. https://10.1016/j.oceaneng.2017.06.020
26. A. Hyvarinen, E. Oja, Independent Component Analysis: Algorithms and Applications, *Neural Netw.*, **13** (2000), 411–430. https://https://doi.org/10.1016/S0893-6080(00)00026-5
27. L. Han, C. W. Li, S. L. Guo, X. W. Su, Feature extraction method of bearing AE signal based on improved FAST-ICA and wavelet packet energy, *Mech. Syst. Signal Proc.*, **62-63** (2015), 91–99. https://10.1016/j.ymssp.2015.03.009
28. G. Stefatos, A. Ben Hamza, Dynamic independent component analysis approach for fault detection and diagnosis, *Expert Syst. Appl.*, **37** (2010), 8606–8617. https://10.1016/j.eswa.2010.06.101
29. L. F. Cai, X. M. Tian, A new fault detection method for non-Gaussian process based on robust independent component analysis, *Process Saf. Environ. Protect.*, **92** (2014), 645–658. https://10.1016/j.psep.2013.11.003
30. J. Yu, A nonlinear kernel Gaussian mixture model based inferential monitoring approach for fault detection and diagnosis of chemical processes, *Chem. Eng. Sci.*, **68** (2012), 506–519.

https://10.1016/j.ces.2011.10.011
31. Y. Deng, Deng entropy, *Chaos Solitons Fractals*, **91** (2016), 549–553. https://10.1016/j.chaos.2016.07.014
32. W. Qiao, D. Lu, A Survey on Wind Turbine Condition Monitoring and Fault Diagnosis-Part I: Components and Subsystems, *IEEE Trans. Ind. Electron.*, **62** (2015), 6536–6545. https://10.1109/tie.2015.2422112
33. O. AlShorman, M. Irfan, N. Saad, D. Zhen, N. Haider, A. Glowacz, et al., A Review of Artificial Intelligence Methods for Condition Monitoring and Fault Diagnosis of Rolling Element Bearings for Induction Motor, *Shock Vib.*, **2020** (2020). https://10.1155/2020/8843759
34. O. AlShorman, F. Alkahatni, M. Masadeh, M. Irfan, A. Glowacz, F. Althobiani, et al., Sounds and acoustic emission-based early fault diagnosis of induction motor: A review study, *Adv. Mech. Eng.*, **13** (2021). https://10.1177/1687814021996915

AIMS Press